ejpmr, 2019,6(10), 121-136

SJIF Impact Factor 6.222

EUROPEAN JOURNAL OF PHARMACEUTICAL AND MEDICAL RESEARCH

www.ejpmr.com

Research Article

ISSN 2394-3211

EJPMR

EVALUATION OF CELL DEATH MECHANISMS INDUCED BY HYPERICIN AND ITS DERIVATIVE IN COLORECTAL CARCINOMA MODELS

Youssef M. Shehata[1], Hala M. Ali[1,2]* and Nermin Raafat[3]

[1]Department of Biochemistry, Faculty of Veterinary Medicine, Zagazig University, Zagazig, 44519, Egypt.
[2]Scientific & Medical Research Center (ZSMRC), Faculty of Medicine, Zagazig University.
[3]Department of Medical Biochemistry, Faculty of Medicine, Zagazig University.

***Corresponding Author: Hala M. Ali**
Scientific & Medical Research Center (ZSMRC), Faculty of Medicine, Zagazig University.
Email Id: halamohamed5521@gmail.com,

Article Received on 07/08/2019 **Article Revised on 27/08/2019** **Article Accepted on 17/09/2019**

ABSTRACT

Colorectal cancer (CRC) is the third most malignancy and the fourth human killer. Photodynamic therapy (PDT) has emerged as a promising alternative to conventional cancer therapies. This study aimed to investigate the ability of Hypericin (HY) and its derivative (HAHY) as synthetic photosensitizers (PSs) to induce tumoricidal effect in HCT-116 carcinoma models. Sixty balb/c male mice were transplanted with 5×105 HCT-116 cells to induce carcinoma bearing mice model. The experimental animals were then divided into five groups; Group I (untreated), Group II (HY-PDT), Group III (HAHY-PDT), Group IV (HY-PDT+EGCG) and Group V (FOLFOX). Blood, liver and tumor mass samples were taken. Also, biochemical studies and MTT assay were performed. HY and HAHY-PDT had a significant cytotoxic effect on human HCT-116 cells. Also, a significant upregulation in gene expression of P53 and CYT-c in concentration dose dependent manner. Furthermore, a significant increase in IL-6 gene expression in group (2) higher than that in group (3).Whereas it decreased in group (5), and showed insignificant difference in group (4) .Also, results showed decrease in VEGF gene expression in both group (3) and (4), while it showed significant increase in group (2) and slight increase in group (5). In conclusion, these PSs possess a strong cytotoxic and apoptotic effect on human HCT-116 cells. Using of EGCG along with HY-PDT improves the outcome. Also, HAHY-PDT can be used as an alternative to HY-PDT, where it showed tumor shutdown without metastasis besides its antitumor immunity.

KEYWORDS: Hypericin; Hexa Acetyl Hypericin; Colorectal cancer; Photodynamic therapy; Synthetic photosensitizers.

INTRODUCTION

Colorectal cancer (CRC) is known to be the fourth most popular cause of cancer-related deaths and the third most frequent cause of malignancy.[1] CRC development is attributed to a combination of genetic and environmental factors.[2] Surgical resection is the main curative choice for patients with metastatic colon cancer. Not all patients are good candidates for surgery, unfortunately.[3] Chemotherapy is often used in these cases FOLFOX (5-fluorouracil / leucovorin and oxaliplatin) are the most widely utilized chemotherapy regimens.[4] FOLFOX has become part of the international routine in adjuvant care and palliative cancer treatment.[5] Oxaliplatin is related to the neurotoxicity found during and after FOLFOX therapy.[6] These traditional methods result in poor quality of life, toxicity, lower overall survival rate, and drug resistance.[7]

Developing new strategies as well as novel agents with lower toxicity and higher efficacy become important.[8] Photodynamic therapy (PDT) is an effective therapeutic approach involving a non-toxic photosensitizer (PS) compound, oxygen (O2) and adequate wavelength light irradiation resulting in selective destruction of tumor cells.[9] The apparent benefits of PDT over traditional therapies are its direct targeting,[10] cheaper process, fewer adverse side effects[11] and decreased toxicity for prolonged treatment.[12] and non-immunosuppressive therapy.[13]

Hypericin (HY), a photosensitizer that occurs naturally synthesized by Hypericum sp. (St. John's Wort), has properties ideal for PDT.[14] It is a second-generation photosensitizer with highly efficient in the synthesis of singlet oxygen and superoxide anions after light wavelength irradiation about 600 nm.[15] and minimal or no toxicity in the dark.[16] Several in vivo and in vitro studies have verified the function of photodynamic hypericin therapy (HY-PDT) against proliferation of tumor cells.[17] While HY is located in the endoplasmic reticulum and Golgi apparatus, not in the mitochondria,[14] accelerated loss of

mitochondrial membrane potential, subsequent release of cytochrome-c, caspase-3 activation and apoptosis occurred as a result of the activated HY photodynamic action.[18] TP53, a tumor suppressor gene, plays a major role in the response of cells and in the defense against DNA damage.[19] P53 incorporates signals as a result of various stimuli such as oxidative stress and hypoxia.[20] Previous work investigated the frequency of HY-PDT evoked cell death in HT-29 colon adenocarcinoma cells of the mut-p53.[21] HY's photosensitizing results are generally considered to be oxygen-dependent.[22] HY-PDT's primary activity is tumor vasculature damage where it induces oxidative stress, contributing to hypoxia in the tumor tissue and allows angiogenic compounds to be released, contributing to angiogenesis. This angiogenesis is mainly due to the increased regulation of cyclooxygenase 2 (COX-2) and the release of proangiogenic factors such as vascular endothelial growth factor VEGF that promote endothelial cell proliferation, migration and tube formation from existing vessels required for tumor growth, progression and metastasis.[23,24] Research have shown that high levels of VEGF found in solid tumors are associated with bad clinical outcomes.[25] Some researchers recorded increased VEGF production after PDT.[26-28] In addition, epigallocatechin-3-gallate (EGCG), a natural COX-2 inhibitor,[29] is a main flavonoid and accounts for half of green tea polyphenols. It has antiangiogenic properties,[30] anticarcinogenic, antimetastatic[31] and chemo-preventive effects.[32] EGCG inhibits cell proliferation and induces apoptosis in colorectal cancer cells.[33] In addition, inflammatory responses caused by reactive oxygen species (ROS) are known to be a crucial priming event in the formation of anti-tumor immunity.[34] The HY-PDT phototoxic reaction initiates the release of proinflammatory mediators by introducing interleukin IL-6 into the tumor microenvironment that induces a powerful inflammatory response.[35] HY-PDT could also facilitate tumor death by producing macrophages and neutrophils. Generally, HY-PDT is considered important for antitumor immune activation.[36] Collectively, this study aimed to test the tumoricidal efficacy and molecular mechanisms of HY-PDT, HexaAcetyl Hypericin (HAHY)-PDT and EGCG along with HY- PDT in comparsion with FOLFOX against HCT-116 colorectal carcinoma models.

2. MATERIAL AND METHODS

2.1. Chemicals

HY and its derivative HAHY were prepared according to Amer et al.[37] and references there in. Also, they were kindly obtained as agift from professor doctor Atef Amer (Fig.1).These materials were dissolved in sterile Dimethyl sulfoxide (DMSO) to prepare a stock solution that was stored at -20^{o}C until further diluted 1x PBS shortly before injection into animal. FOLFOX was obtained from the National Cancer Institute (NCI), Cairo University. EGCG was obtained from the company of Now Foods (Bloomingdale, IL60108, USA, nowfoods.com).

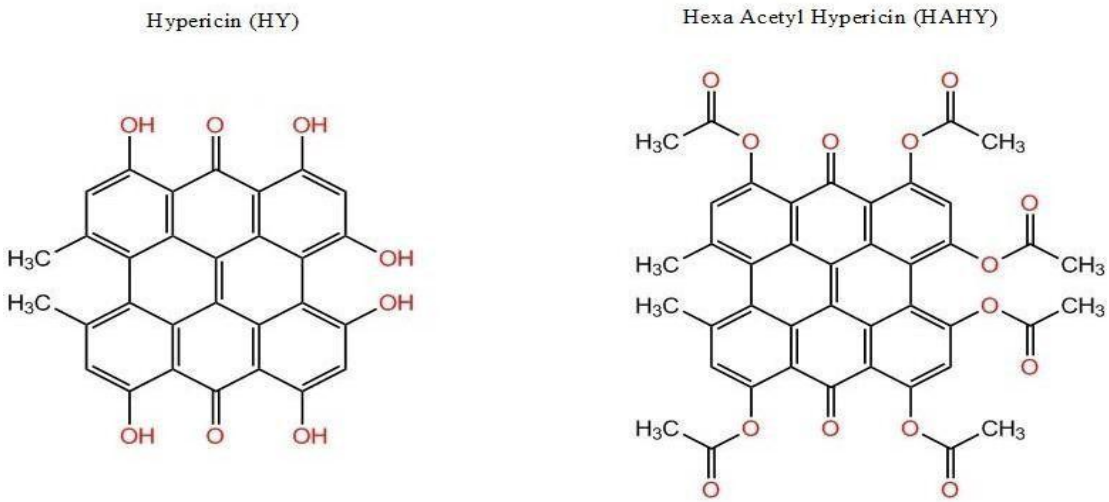

Figure 1: Chemical structure of HY and HAHY and its Molecular weights: 504 and 756 respectively.

2.2. Gas Chromatography –Mass Spectrometry

The procedure was conducted in Micro Analytical center, Cairo University. The sample was analyzed by (C:/GCMS solution) negative ion acquisition mode on DI Anyalysis Shimadzu QP-2010 Plus instrument. The program was operated as follows: start time: 0 min, end time: 10.00 min and the event time were held for 0.50 sec. The parameters for analysis were carried out using negative ion mode as follows: Ion source temperature 250 ^{o}C, Electron voltage 70eV and scan speed: 1666. Mass spectra were detected in the ESI negative ion mode between m/z 50–800. The peaks and spectra were processed using the Maslynx 4.1 software and tentatively identified by comparing its retention time (R) and mass spectrum with reported data.

2.3. In vitro PDT treatment

HY and HAHY were dissolved in DMSO and stored at -20^{o}C, dilution was made using DMEM containing 0.1 % (v/v) DMSO as final concentration.HCT-116 cells

(5x105) cells / ml were seeded on six well culture plate containing 2 ml DMEM, 24 hrs after incubation, the medium was removed and fresh medium containing various concentration of HY (0.25-0.5-1µg /ml) and HAHY (10-15-25 µg/ ml) were added and incubated for 16 hrs in the dark and one well was seeded without drug as untreated control. After PDT treatment, cells were incubated in dark for 24 hrs at 37^{o}C in humified atmosphere of 95%, 5% CO2 until further analysis. The collected HCT-116 cells were used to study p53 and Cytochrome -c (CYT -c) genes expression using RT-PCR.

2.4. Cytotoxic effect on HCT-116 cell line using MTT assay

This cytotoxic activity test was conducted and determined in the Bioassay Cell Culture Laboratory, National Research Centre, Dokki, Egypt. The MTT assay is a colorimetric assay depend on reduction of yellow MTT (3- (4,5- dimethylthiazol-2-yl) -2,5- diphenyl tetrazolium bromide) to purple formazan. Briefly, l04cells/well were treated with various concentrations of HY and HAHY for 16 hrs in dark followed by PDT.

After 24hrs of incubation following PDT treatment, 2.5µg/ml of MTT was added to each well and incubated at 37°C for 4hrs. The formazan crystals that were formed were dissolved by adding 200 µl/well of 10% Sodium dodecyl sulphate. A positive control was used that gives 100% lethality under the same conditions and the absorbance was read at 595 nm.

The percentage of change in viability was calculated according to the formula: (Reading of tested compound / Reading of negative control) -1) x 100.[38]

2.5. Induction of tumor bearing mice model

Sixty balb/c male mice (8-10 weeks old) weighting 25 gwere obtained from the Animal House of ZSMRC, Zagazig University, Egypt. They were housed in a temperature-controlled and light-controlled room (12 h light/dark cycles) with free access to food and water. The human epithelial colorectal carcinoma cell line HCT-116 (purchased from VACSERA, Giza, Egypt) was used to establish the HCT-116 bearing mice model.[39] The cells were cultured as a monolayer in DMEM medium supplemented with 10% fetal bovine serum and 100 units/ml penicillin/streptomycin and incubated at 37°C,95% humidity, and 5% CO2 (NÜVE CO2 incubator). The cells were examined under inverted microscope (Leica). Once confluent, the cell layer was washed with phosphate-buffered saline (PBS), trypsinized, and counted using a hemocytometer. Before inoculation, approximately 5×105cells were suspended in PBS and injected subcutaneously into the lower left flanks of the 60 mice.[40] All experimental procedures were performed according to the guidelines of the Institutional Animal Care and Use Committee of the Zagazig University.

2.6. In vivo treatment protocols

Two weeks after inoculation, different treatment protocols have started and continued for 4 weeks. The animals were randomly assigned to five different groups (n=12) for treatment: Group1; control (mice with untreated tumor). Group 2; treated intraperitoneally (IP) with 5mg/kg B.wt HY.[41] Group 3; treated IP with 5mg/ kg B.wt HAHY .Group 4; treated IP with 2 mg/kg B.wt HY[28], in combination IP with 50 mg/kg B.W EGCG.[42]

Group 5; treated with (IP) 6mg/kg oxaliplatin and after 2hrs with 50mg/kg B.wt (5-Fu) + 90mg/kg B.wt leucovorin.[43] The experimental animals in each of the treated groups (2, 3, 4), 2 hrs after injection, were irradiated for 5 min[41] by exposure of the tumor area of mice to 7L18w/30 fluorescent lamps for 5 days a week.[44]

2.7. Sampling

At the end of the experimental period, all animals were sacrificed and venous blood samples were collected from the retroorbital plexus on EDTA, tumor mass and liver tissue samples were taken for biochemical and histological studies.

2.8. RNA extraction, cDNA synthesis and real time RT-PCR

Total RNA was extracted from the culture collected cells, from the tumor tissue homogenate and from whole blood of mice bearing HCT-116 cell using PureLink® RNA Mini Kit purchased from Ambion by life technologies by Thermo Scientific, Catalog numbers: 12183018A following the manufacture instructions. cDNA was synthesized using a High Capacity cDNA Reverse Transcription Kit purchased from Thermo Scientific, code 40374966. Real time PCR amplification was performed using Maxima SYBR Green qPCR Master Mix (2X) kit purchased from Thermo scientific, catalog #K0251. PCR reactions were incubated for 10 min at 95 ^{o}C as initial denaturation and polymerase activation, after which the target was amplified with 45 cycles for 15 sec at 95^{o}C as denaturation and 30 sec at 51^{o}C as annealing and 30 sec 72^{o}C as extension, this program was operated by Stratagene Mx3005P. The amount of target gene expression levels was quantified using the formula $2^{-\Delta\Delta ct}$.[45] The gene expression level was normalized to GAPDH. The primers used were purchased from Invitrogen Thermo Scientific as shown in Table 1.[9,46-49]

Table 1: Specific primers for examined genes.

Genes	Primers
hCYT-C	5`- AGTGTTCCCAGTGCCACACCG-3`
	5`-TCCTCTCCCCAGAATGATGCCTTTG-3`
hGADPH	5`-AAGGTGAAGGTCGGAGTCAAC-3`
	5`-GGGGTCATTGATGGCAACAATA-3`
hP53	5`-ACTTGTCGCTCTTGAAGCTAC-3`
	5`-GATGCGGAGAATCTTTGGAACA-3`
mVEGF	5`-GTGAGGTGTGTATAGATGTGGGG-3`
	5`-ACGTCTTGCTGAGGTAACCTG-3`
mIL-6	5`-CTGCAAGAGACTTCCATCCAG-3`
	5`-AGTGGTATAGACAGGTCTGTTGG-3`
mGADPH	5`-TGGCCTTCCGTGTTCCTAC-3`
	5`-GAGTTGCTGTTGAAGTCGCA-3`

2.9. Histological and immunohistochemical study

Tumor mass and liver from each animal was carefully dissected and the specimens were immediately immersed in 10% neutral buffered formaline for 48 hrs before being processed to prepare 5-µm-thick paraffin sections and stained with hematoxylin and eosin (H & E). The immunohistochemical staining occurred by using Cytokeratin7 to investigate the origin of this study tumor cell in both liver and lymph node of untreated group which were bearing to HCT-116 cell line. Slides were viewed by using Labomed,Labo America, Inc. USA microscope.[50]

2.10. Statistical analysis

Data were statistically analyzed using the software SPSS. One-way ANOVA was used to analyse the variance, and dunken post hoc test Multiple Comparison test was used to compare the genes expression levels in all the groups. Data were mean± SEM, *P<0.05, **P<0.001, ***P<0.001 and ns>0.05.

3. RESULTS

3.1. **Gas Chromatography –Mass Spectrometry Result**

Gas chromatography–mass spectrometry (GC-MS) is a hybrid analytical technique that couples the separation capabilities of GC with the detection properties of MS to provide a higher efficiency of sample analyses. While GC can separate volatile components in a sample, MS helps fragment the components and identify them on the basis of their mass. The major advantage of this technique is its selectivity and its capability to give information about the structure of the tested compound. From this point of view the analysis of synthetic Hexa Acetyl Hypericin (HAHY) is carried out using thisadvanced analytical technique of chromatography coupled to electrospray ionization mass spectroscopy (C:/GCMS) in negative mode to confirm its structure and Molecular weight.

This type of scan displays one and two masses unit higher than the initial mass of the tested compounds (M+1) and (M+2). The x-axis represents the expanding mass-to-charge (m/z) ratio whereas the y-axis shows the relative abundance of each ion which is associated to the number of times that an ion of that m/z ratio hits the detector. (Fig.2) shows the the total ion MS spectrum of HAHY. The molecular ions (M+1) at m/z757 and (M+2) at m/z 758 were displayed by HAHY in the negative ion mode. The fragment at m/z743 (M+1-CH2) was observed. The fragment at m/z 674 (M+2-2CH2=C=O) resulted from the loss of the diacetyl groups and represents tetraacetyl Hypericin. The fragment at m/z 587(M+1 -2CH3-C=O-2CH 2=C= O) resulted from the loss of the tetraacetyl groups and represent diacetyl Hypericin. The peak at m/z 504 (M-6CH2=C=O) resulted from the loss of the hexaacetyl groups and represents Hypericin. Product ions of m/z 252 and 142 were also detected which represents Emodine and the compund resulted from losing C7H8O from Emodin respectively. The base peak at relative intensity 100% was detected at m/z 57.

These results proved that the tested compound is Hexa Acetyl Hypericin and it has the molecular weight equal to 756.

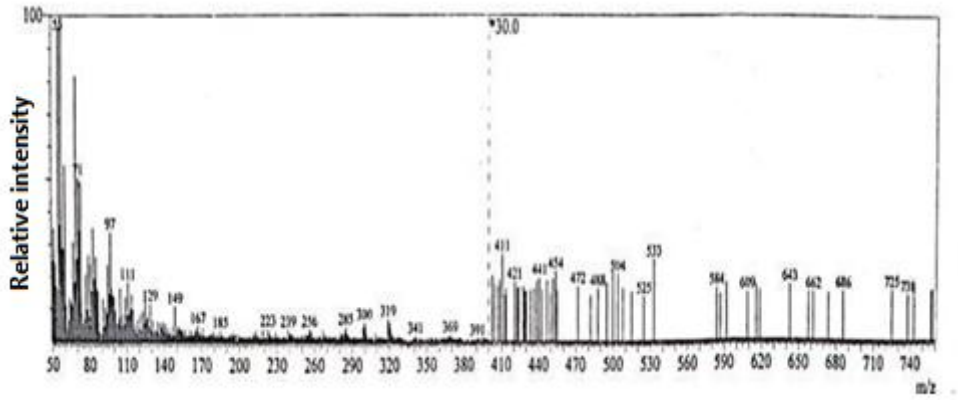

Figure 2: Fragment ions MS spectrum of HAHY.

3.2. Invitro Model Results

3.2.1. Cytotoxic effect of HY and HAHY - PDT on HCT-116 cell line

The MTT assay was performed to assess the rate of proliferation of HCT-116 cells after treatment with varying concentrations of HY and HAHY-PDT ranged between 0.78 to 100 µg/ml. The result showed that the current PSs inhibited the growth of HCT-116 cells in a concentration-dependent manner. At the concentration of 2.03µg/ml for HY, 50% viability was detected during the 48 h treatment, whereas maximum cytotoxicity LC90 was observed at a concentration of 5.5µg/ml. Whereas at the concentration of 52.3µg/ml for HY derivative, 50% viability was detected, and maximum cytotoxicity LC90 was observed at a concentration of 82.5µg/ml as showed in table (2) and (Fig.3).

Table 2: LC50 & LC90 of HY and HAHY on HCT 116 cells lines by using MTT assay.

Sample	LC50	LC90	Remarks
HY-	2.03	5.5	100% at
HAHY-	52.3	82.5	95.2% at

LC50: Lethal concentration of the sample which causes the death of 50% of cells in 48 hrs. LC90: Lethal concentration of the sample which causes the death of 90% of cells in 48 hrs.

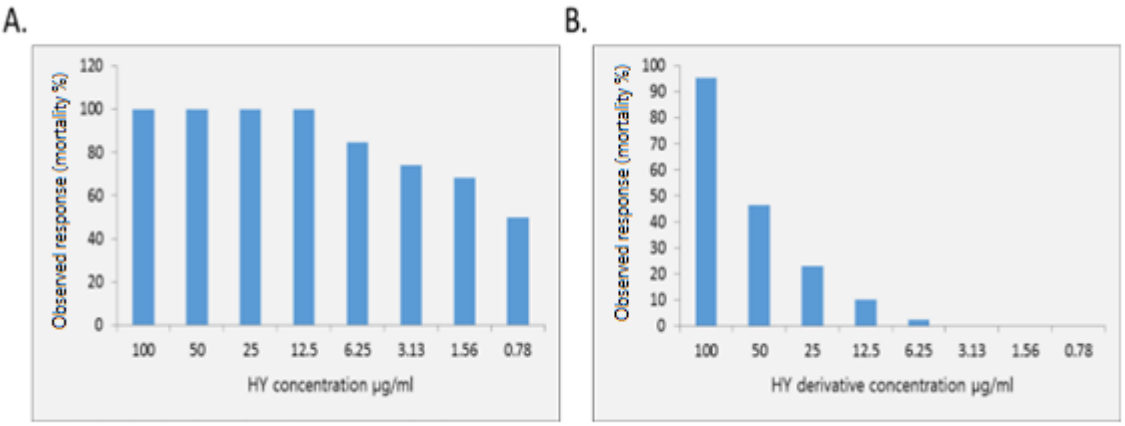

Figure 3: The effect of different concentration of HY (A) and its derivative (B) on HCT 116 cell line viability by using MTT assay.

3.2.2. Effect of HY and HAHY-PDT on p53 and CYT-c genes expression using RT- PCR

The results of genes expression showed increase in the level of P53 gene expression in HCT 116 cells by increasing the concentration of all treated groups compared with the untreated group. While, CYT-c gene expression was significantly elevated with increasing the concentration in all treated groups except the concentration of 10 µg/ml HY derivative-PDT in HCT 116 cells (figure4).

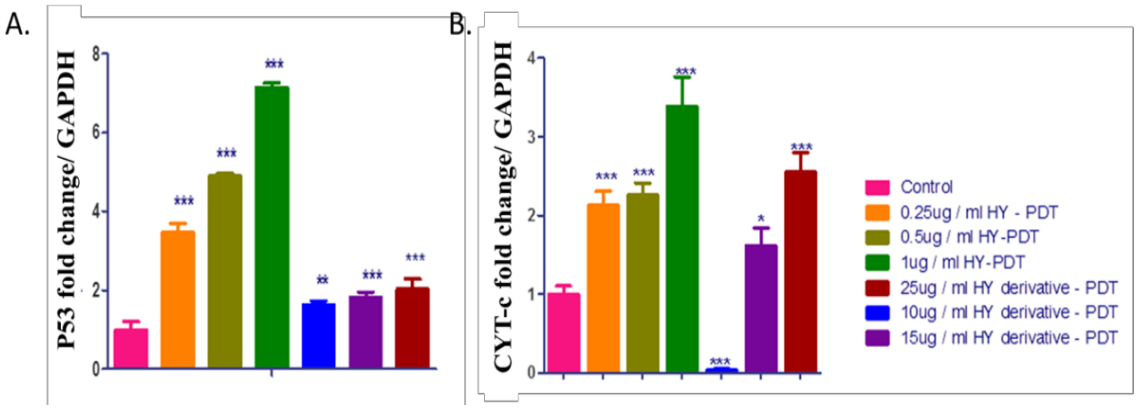

Figure 4: P53 (A) and CYT-c (B) genes expression of vitro model in untreated, HY (0.25, 0.5 and 1 µg/ml) and HY derivative (10, 15 and 25 µg/ml) treated HCT 116 cell line, gene expression analysis was performed at 24 post PDT treatments. Data are mean±S.E.M. statistically significant difference were labeled as *P<0.05, **P<0.001, ***P<0.0001 and ns>0.05, ns is non-significant.

3.3. Invivo Model Results

3.3.1. HY and HAHY mediated PDT lead to up regulation of IL-6 in HCT-116 bearing mice resulting in anti-tumor immunity

There was a highly significant increase in IL-6 expression of tumor mass in group (2). While, there were slight significant increase in group (3). There were a highly significant increase in IL-6 expression of blood samples in group (2), while there were non-significant difference in group (3) compared with untreated group (control) as shown in figure (5B and C).

3.3.2. Effect of HY and HAHY mediated PDT on VEGF in HCT-116 bearing mice

There was a highly significant increase in VEGF expression of tumor mass in group (2). While, there were slight significant decrease in group (3) treated with the same dose with HAHY-PDT compared with untreated group as shown in figure (5A).

3.3.3. Effect of EGCG treated along with HY-PDT as anti-angiogenesis on VEGF expression and as anti-inflammatory on IL-6 expression

In present study, we used EGCG along with HY-PDT. Our results showed significant decrease in VEGF of tumor mass. While this group showed non-significant difference in IL-6 of tumor mass. Whereas there were a significant decrease in IL-6 of blood samples of this group in comparison with control group as shown in figure (5A-C).

3.3.4. Effect of FOLFOX on VEGF and IL-6 genes expression in HCT -116 bearing mice

There were a little significant decrease in IL-6 gene of tumor mass in group (5) treated with FOLFOX with non-significant difference in IL-6 gene of blood samples. Whereas there were a little significant increase in VEGF gene of tumor mass of this group in comparison with untreated group as shown in figure (5A-C).

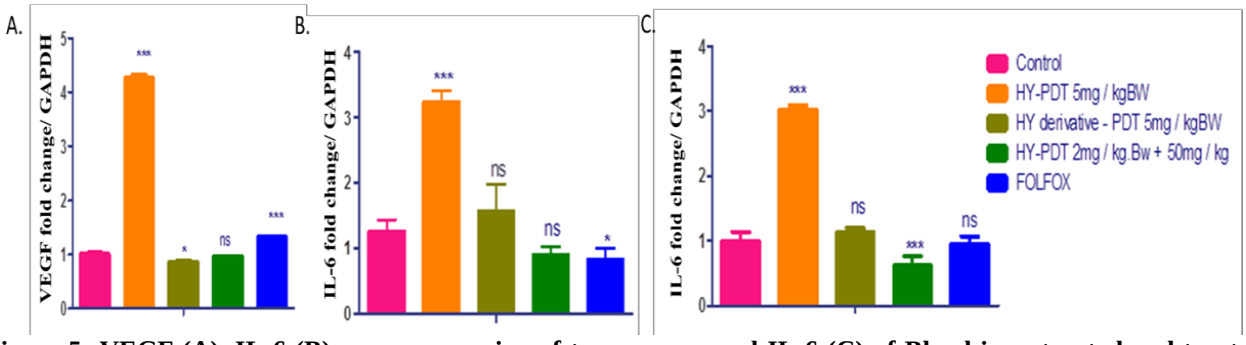

Figure 5: VEGF (A), IL-6 (B) genes expression of tumor mass and IL-6 (C) of Blood in untreated and treated groups of HCT -116 cell line bearing mice. Data are mean ± S.E.M. Statistically significant difference were labeled as *P<0.05, **P<0.001, ***P<0.0001 and ns >0.05, ns is non-significant.

3.4. Immunohistochemistry Results

In group (1), immunohistochemically (IHC), both liver and L.N of this group showed strong positive reaction with Cytokeratin 7 as brown coloration occupying the cytoplasm of the metastatic cells of both liver and L.N. denoting an epithelial origin of such tumor cells confirming that the detected tumor in this organs was HCT -116 colorectal carcinoma (Fig.6 A and B).

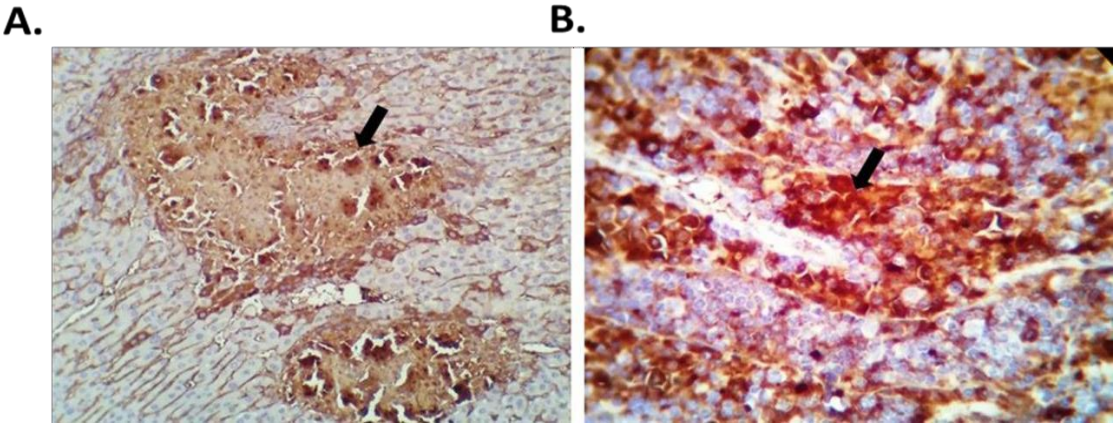

Figure 6: Metastasis of HCT-116 cell line in liver and lymph node of the untreated group (A&B). A Photomicrograph of immunostained section for Cytokeratin 7 of control mice lymph node H&E x400. B. A Photomicrograph of immunostained section for Cytokeratin 7 of control mice liver H&E x400.

3.5. Histopathological Results

In group (1), H&E staining showed that Examined sections from subcutaneous lymph node (L.N.) appeared with replacement of nodal architecture by groups and nests of atypical large polygonal epithelial cells with intact nodal capsule (Fig.7A). Liver sections of this group showed dilated congested central vein and sinusoids; scattered hepatocytes showing hepatocellular dysplasia; and scattered foci of malignant epithelial cells mainly at the surface showing hyperchromatic nuclei and increased mitosis and mild lobular inflammatory infiltrate (Fig.8A).

In group (2), H&E staining showed that L.N sections presented as normal lymphoid structures free of neoplastic metastasis also, replacement of lymphoid tissue by polymorphous infiltrate of non-specific inflammatory cells (Fig.7B). Liver sections of this group revealed focal vascular metastasis of atypical epithelial cells, portal and interstitial chronic inflammatory cell aggregation of round cells, kuffer cells hypertrophy and degenerative changes in some hepatocytes and replacement of portal triad by non-specific inflammatory cells (Fig.8B).

In group (3), H&E staining showed that L.N. revealed normal cortical and medullary structures. No tumor cells could be observed. (Fig.7C). Liver section of this group revealed congested portal blood vessels inflammatory cells infiltration and mild biliary proliferation. No tumor cells could be detected (Fig.8C).

In group (4), H&E staining showed that L.N revealed cortical and medullary lymphoid hyperoplasia with predominant plasma cell reaction (Fig.7D). Liver section of this group revealed Lymphocytic hepatitis as demonstrated by aggregation of moderate number of lymphocytes in the portal triade with mild biliary proliferation (Fig.8D).

In group (5), H&E staining showed that L.N was in normal cortical and medullary structures free from any tumor metastasis (Fig.7E). Liver sections of this group revealed normal hepatic parenchyma. No evidence of tumor metastasis or liver degenerative changes or mild to moderate hepatitis could be detected (Fig.8E).

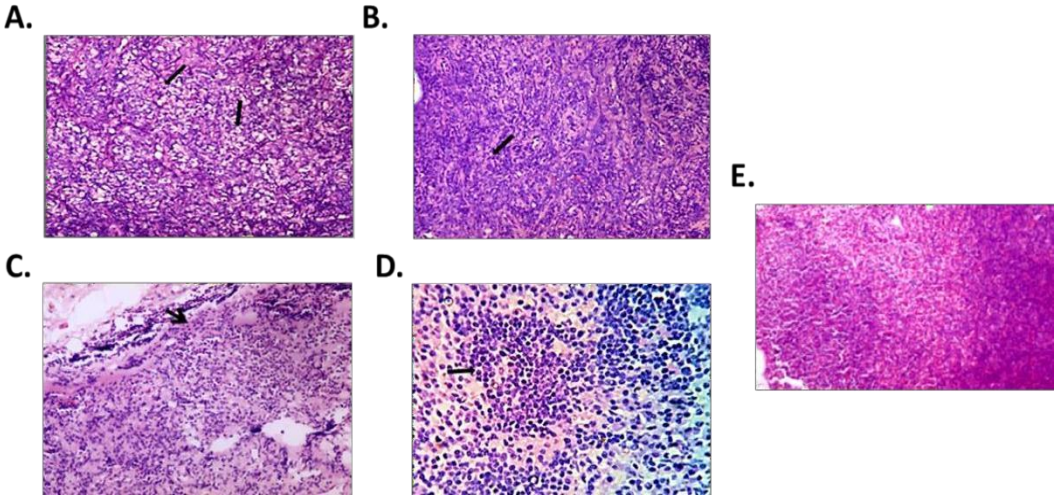

Figure 7: Effect of HY, HAHY, HY+EGCG and FOLFOX on lymph node morphometry of different treated groups (A – E). A. Photomicrograph of control mice lymph node showing: replacement of nodal architecture by groups and nests of atypical large polygonal epithelial cells (black arrow), H&E x400. B. Photomicrograph of HY treated mice lymph node showing distorted nodal architecture and desmoplastic reaction with no evidence of neoplastic infiltration (black arrow); H&E x 400. C. Photomicrograph of HAHY treated mice lymph node showing replacement of lymphoid tissue by polymorphous infiltrate of non-specific inflammatory cells mainly; H&E x400. D. Photomicrograph of HY+EGCG treated mice lymph node showing cortical and medullary lymphoid hyperplasia with predominant plasma cell reaction (black arrow) H&E x400. E. Photomicrograph FOLFOX treated mic lymph node showing normal cortical and medullary structures free from any tumor metastasis H&E x400.

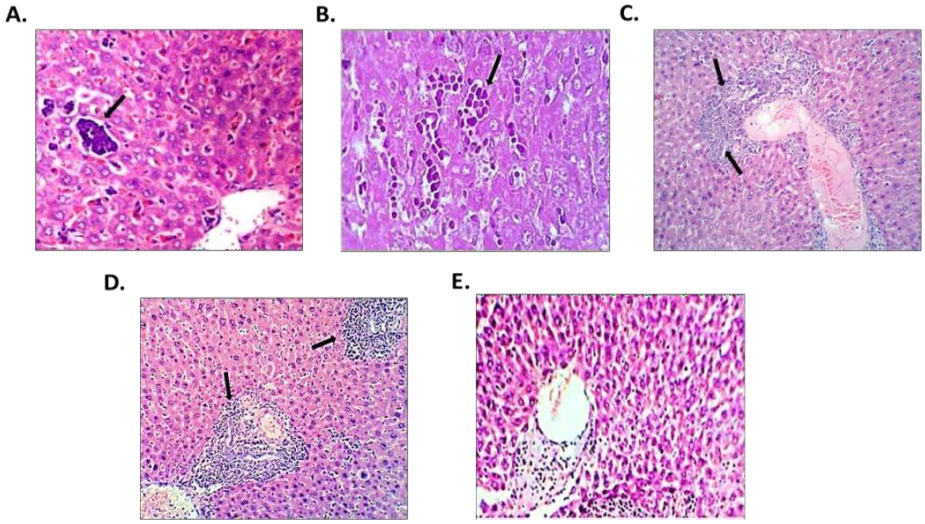

Figure 8: Effect of HY, HAHY, HY+EGCG and FOLFOX on liver morphometry of different treated groups (A-E). A. Photomicrograph of control mice liver showing focal invasion of liver tissue by groups of atypical large polygonal epithelial cells with hyperchromatic nuclei; H&E x400. B. Photomicrograph of HY treated mice liver showing focal vascular metastasis of atypical epithelial cells (black arrow) H&E x400. C. Photomicrograph of HAHY treated mice liver showing congested portal blood vessels, inflammatory cells infiltration and mild biliary proliferation (black arrow) H&E x400. D. Photomicrograph of HY+EGCG treated mice liver showing Lymphocytic hepatitis as demonstrated by aggregation of moderate number of lymphocytes in the portal tirade with mild biliary proliferation (black arrow) H&E x400. E. Photomicrograph FOLFOX treated mice liver showing normal hepatic parenchyma. No evidence of tumor metastasis or liver degenerative changes or hepatitis H&E x400.

4. DISCUSSION

The second most common cancer among males is colorectal cancer and represents the third most common cancer among women in the world. This triggers cumulative cancer-related deaths.[51] The only possible cure is surgical resection. It has been shown that post-operative adjuvant chemotherapy enhances results.[52]

FOLFOX has become the popular adjuvant treatment for the management of stage III colon cancer, which results

in significant increases in cost and toxicity. In total, 92.1 percent of patients receiving treatment were registered for oxaliplatin-induced neurotoxicity, peripheral neuropathy.[53] There is therefore a great need to explore potential CRC care methods.

Photodynamic therapy (PDT) is a cancer treatment technique that targets non-toxic photosensitizer preferentially found in tumor tissue and its directed activation with light, resulting in the corresponding release of reactive oxygen species inducing three photochemically mediated cell death mechanisms.; direct cellular toxicity, tissue anoxia with tumor hunger due to ROS-mediated tumor vasculature shutdown d from the plant Hypericum perforatum, was used in PDand antitumor immune response.[54] Hypericin (HY), obtaineT due to preferential aggregation in cancer cells, higher quantum yields and low dark cytototoxicity.[9] Many in vitro and in vivo studies in colon cancer cells reported an antiproliferative impact of HY.[55-56]

The choice of HY-PDT was according to Paszkoa *et al*.[57]; Yoo and Ha,[58] Who mentioned that several PSs, including HY, are in advanced phases of clinical trials or in the phase of approval for the treatment of several malignancies. PDT has been approved to treat bladder, head and neck, lung, breast, esophageal, cervical and pancreatic cancers in several countries, but its clinical use and treatment of other types of cancer, including colon cancer, still have loose ends. In fact, since tumor tissues have properties such as decreased pH and high lipid content, it leads to the favorable aggregation of PSs in tumors by enhanced permeability retention (EPR) effect and is thus passively absorbed so that their selective absorption can be accomplished, facilitating PDT-induced tumor degradation with only minimal healthy tissue harm. [59] In addition, HY has a high affinity for cancer cells due to the high content in cancer cells of low-density lipoprotein (LDL) receptors which enhances PS uptake.[11]

For these reasons, we shed light on the therapeutic effect of HY-PDT with different concentrations in vitro and in vivo HCT-116 models. This study differs from others where, we used for the first time HY derivative (HAHY) as a synthetic PS, and also for the first time used EGCG along with HY then compares between its therapeutic effects and that of HY and finally compares between their effects and that of FOLFOX in HCT-116 bearing mice model. This study investigated if the current PSs could induce the three known tumoricidal mechanisms of PDT in HCT-116 models.

The present study revealed the cytotoxic effect of current PSs on HCT-116 cell line using MTT assay confirming the first tumoricidal mechanism of PDT using HY and HAHY.

These findings were confirmed by the Blank et al.[60] experiment which concluded that,by using an MTT assay, HY-PDT had significant cytotoxic activity at low dose against Murine C 26 colon carcinoma, showing that LC50 was 1µM.

In addition, it was supported by Sačková et al.[55] who confirmed that HY-PDT had antiproliferative activity in CRC cells.

Our findings were in line with Mikes et al.[61],who revealed a dose dependent reaction to HY-PDT which was significant in almost all groups comparing to untreated control when examining HY-PDT's in vitro cytotoxic activity on HCT-116 cell lines by MTT assay. Another studies demonstrated the strong cytotoxic impact of HY using MTT assay on cell lines HT-29 and Caco-2.[62]

The mechanism of this selective cytotoxic and apoptotic effect of current PSs was studied through detection of the expression of some apoptotic genes such as P53 and CYT-c. The results showed that the mRNA expression levels of these genes were significantly increased according to their concentrations which indicate the apoptotic effect of them on HCT-116 cell line.

Our results have been confirmed by multiple studies. Sanovic et al.[56] revealed that ROS-derived photochemical oxidation by type I and type II resulting in oxidative stress and, in the event of excessive damage or stress, cell death occures through apoptosis where this was in line with our results where our PSs generated ROS by type I and type II photochemical reaction as previously proved by Plaetzer et al.,[63] and Van Golen et al.[64] Turrens,[65] has shown that in mitochondria, photoactivated ROS induces the release of CYT-c which further activates pro-apoptotic caspases. Another research by Liu et al.[66] found that HY-PDT resulted in the loss of integrity of the mitochondria membrane contributing to the release of CYT-C into the cytosol that interacts with apoptosis protease-activating factor-1 to form apopotsomes, activating caspase 9 and then caspase 3.

Finally, our findings were in line with Du et al.[67] who stated that HY-PDT mediated ROS releasing ca+2 from the endoplasmic reticulum and losing the integrity of the mitochondrial membrane and releasing CYT-C contributing to tumor cell death through the apoptotic mitochondrial pathway.

In our vitro model, we studied also the P53 gene expression, our results showed significant increase in all treated groups with increasing the concentration of HY and its derivative mediated-PDT, Our results were in agreement with Fisher et al.[68]; Tong et al.[69] and Hajri et al.[70], all of whom found that PDT- treated cells with different sensitizers upregulated P53, but PDT- induced death and apoptosis of cells did not demonstrate a significant dependence on P53.

Firstly,in our vivo results, we successes to establish metastasized xenografted model by transplanting $5x10^5$ HCT-116 cells to balb/c mice as shown in and confirmed this with H&E and immunohistochemical investigations in L.N. and liver sections of this group as shown in (Fig.6A and B)which showed strong positive reaction with Cytokeratin 7 denoting an epithelial origin of such tumor cells confirming that the detected tumor in this organs was HCT -116 colorectal carcinoma and this results were in agreement with Rajput *et al.*[39] Whom proved that an epithelial morphology of HCT-116 cells and it can metastasize in xenograft models.

The present study revealed also the second and third tumoricidal mechanisms of PDT using HY and HAHY as synthetic PSs through detection of VEGF and IL-6 gene expression in tumor mass and examination of H&E sections in tumor mass and liver tissues of HCT-116 bearing mice. Our results showed significant increase of VEGF gene expression in tumor mass of group (2) as a result of hypoxia with some metastasis in the liver of this group. This results may be explained by the fact that Present PSs following PDT caused a lack of oxygen in the treated tissue due to the intake of oxygen during PDT in the tissue microvasculture resulting in extreme tissue hypoxia and anoxia, which is known to be the second PDT tumoricidal mechanism in which the stimulation of local hypoxia in the irradiated tumor bulk as a result of O2 consumption in consequence to the $O2 \rightarrow 1O2$ or O2 conversion and oxidation of biomolecules during PDT as well as the shutdown of tumor vasculature after PDT. Under hypoxic stress, adaptive reaction may be accomplished by inducing a hypoxia-inducible factor such as HIF-1α, up-regulating COX-2 that produces PGE2 that leading to releasing of pro-angiogenic signals such as VEGF which enhances migration and differentiation.[71] Our result confirmed with H&E investigation of liver section of this group which showed in (Fig 8B) some focal vascular metastasis of atypical epithelial cells whereas its lymph node section showed normal lymphoid structure free of neoplastic metastasis in (Fig.7B).

Multiple studies confirmed our results: Chen *et al.*[40] found that HY-PDT induced tumor vasculature damage that occurs due to oxygen consumption during PDT triggering oxygen depletion in the treated tumor and lack of nutrients.

Chen, *et al.*[72] found that the bulk of second-generation photosensitizers are distributed mainly in endothelial cells as well as tumor cells that form the tumor vasculature damage, these findings collaborated with Our results for hypoxia induction where our drugs are second-generation and endothelial photosensitizers, as Chen and Witte had previously shown. [73]

Ferrario and Gomer,[27] stated that PDT in treated lesions induced significant increases in VEGF, suggesting that tumor hypoxia plays an important role in angiogenesis. Our tests, however, showed a decrease in the VEGF gene in group (3) treated with HAHY-PDT and also a significant decrease in group (4) treated with HY-PDT in combination with EGCG as COX-2 inhibitors. Whereas there was a slight increase in group (5) treated with FOLFOX relative to the untreated group. This observation was supported by the H&E analysis for the last three groups (3), (4), (5), where there was no indication of tumor metastasis in the liver or lymph node as shown in (Fig.7C-E and Fig.8C-E). This result revealed that the combination of EGCG with HY-PDT enhances the outcome in HCT-116 bearing mice by suppressing the VEGF signaling pathway and inhibiting metastasis to eventually achieve long-term tumor control.

Our results are in agreement with Ferrario *et al.*[74] and Makowski *et al.*[75] who stated that blocking COX-2 with celecoxib showed an increase in mice survival in which specific tumor cell lines were xenografted. Furthermore, our findings were confirmed with Ferrario et al.[76-77], who reported that enhancing PDT with NSAIDS led to a decrease in cell survival in a variety of tumor cell lines with a decrease in PGE2 and proangiogensis factor VEGF rates.

Our results supported with Bhuvaneswari *et al*.[28] which found that the use of celebrex as NSAIDS, together with HY-PDT reduced VEGF expression, indicating that the use of angiogenesis inhibitor may enhance HY-PDT in nasopharyngeal carcinoma.

Eventually, Bhuvaneswari et al.[78] achieved similar positive results when using mAb (Avastin, bevacizumab) against VEGF in parallel with hypericin-PDT on carcinoma tumors of the mice bladder.

Regarding to EGCG, in recent years, several studies are in agreement with our results where Siddiqui *et al.*[79]; Honicke *et al.*[80] and Kwak *et al.*[81], all of whom have shown that EGCG prevents angiogenesis-related biomarkers (e.g. VEGF, angiopoietin1and2), invasion and metastasis (MMP-2, 3, and 9). We also agree with Wu et al.[82], who reported that EGCG increased chemotherapy efficiency in tumor weight and/or volume reduction in xenograft models.

Consequently, the inhibition of COX-2 production with natural inhibitor like EGCG used in our research could be a beneficial intervention technique for PDT to minimize the survival of tumor cells and potentially reduce the proangiogenic impact of PGE2 and preventing metastasis.

Our in vivo findings also revealed that HY and HAHY-PDT may induce antitumor immune response, where our experiments clearly demonstrated that HY and HAHY-PDT with the same dosage contribute to an enhanced release of the IL-6 gene in the tumor microenvironment, which serves as an inducer of chronic inflammation in

addition to different cellular immune responses to damaged cells.

There was a very significant increase in blood sample IL-6 production in group (2), while there was a non-significant difference in group (3), whereas in group (4) treated with HY-PDT + EGCG there was a non-significant difference in IL-6 in tumor mass with a significant decrease in IL-6 of blood samples. While in group (5) treated with FolFox, tumor mass decreased slightly inIL-6 with no significant difference in blood sample geneIL-6 relative to untreated group. Such effects can be clarified by the evidence that PDT mediated inflammatory reactions that lead to tumor vascular damage where phototoxic disruption in tumor blood vessels is a proinflammatory signal perform endothelial cell contraction and basement membrane distribution in the lining of the vessel.[83]As a result, circulating neutrophils and platelets are attracted and attached to lesions resulting in a progressive impairment of vascular function and release of various inflammatory mediators, including leukocyte chemoattractants, cytokines, growth factors and other immune systems.[84]

The characteristic of the inflammatory process is the aggregation of inflammatory cells, including neutrophils, mast cells monocytes / macrophages, which are activated by the release of PDT-treated tumor potent mediators following neutrophil invasion.[85]

Our results in group (2) confirmed by non-specific inflammation in its H&E investigation (Fig.7 B) and, that of its derivative in group (3) also confirmed with some non-specific inflammation in H&E investigation (Fig.7C) which proved that the HY derivative induced slower immuno response than that induced in group (2) treated with the same dose with HY-PDT.

These results supported with Korbelik and Cecic,[86] who confirmed that monocytes / macrophages were another type of non-specific immune response cells contributing to PDT's antitumor impact.

Our results are in line with previously published findings that identified the increased presence of IL-6 in the tumor microenvironment following PDT; Moor et al.,[87] stated that PDT may improve the permeability of the local vasculature by generating proinflammatory cytokines leading to diapedesis of inflammatory leucocytes to the region of inflammation. Also, Gollnick et al..*[88]* had stated that experiments on human cervical carcinoma cells showed evidence that PDT could enhance IL-6 expression after activation of the protein-1 activator.

Furthermore Gabay.[89] stated that PDT can induce certain heat-shock proteins, such as heat-shock protein 70 and heat-shock protein 90, to promote the recruitment of tumor-specific T-cells.

Kabingu [90] demonstrated the third tumoricidal mechanism of PDT which involving the induction of antitumor immune response, where tumor cell death that occurs directly as a result of photochemical damage or as a result of vascular shutdown-mediated hypoxia / anoxia and hyponutrition is the key precursor event for the immune response of the antitumor.

Thong *et al.*[91] reported that the major advantage of PDT-triggered on immunological pathways is that these pathways may trigger an antitumor immune response mediated by antigen-specific T-cells against distant tumor cells that have not been subjected to PDT.

Trisciuoglio *et al.*[92] provided clear evidence to support our observations that HY-PDT contributes to tumor microenvironmental changes by up regulating IL-6 causing chronic inflammation, respectively, culminating in tumor cell death.

Firczuk *et al.*[93] stated that IL-6 as a pro-inflammatory cytokine induced a rapid and strong inflammatory response. Such pathways, together with the release of histamine and serotonin from destroyed vasculature, induce tumor site invasion by the stimulation of different immune cells (neutrophils, mast cells and macrohages) that become stimulated and causes the death of tumor cells.

Moreover, Zhao *et al.[94]* had provided evidence that IL-6 could be increased by subcutaneous tumors following PDT.

He *et al.*[95] illustrated that PDT triggers oxidative stress that produces defensive reactions including the expression of heat shock proteins (HSPs), transcription factors such as nuclear factor kB (NF-kB) and activator protein 1(AP-1) then induce immunoregulatory and proinflammatory protein production such as IL-6 interleukins.

Lastly Barathan *et al.*[9] found that IL-6 had dramatically increased in HepG2 cells treated with 1µg/ml HY-PDT resulting in cell death providing additional hints to the presence of potential antitumor immune pathways in hepatocellular carcinoma.

5. **CONCLUSIONS**

In summary, there can be no doubt that FOLFOX has increased survival of colorectal cancer patients with metastatic disease, but still has neurotoxicity as a side effect. The current PSs have a strong cytotoxic and apoptotic effect on human HCT- 116 cells. Combining HY-PDT and EGCG is a promising approach for cancer therapy, in agreement with previous preclinical studies involving angiogenesis inhibitor combination therapies. Also, HAHY-PDT can be used as an alternative to HY-

PDT, where it showed tumor shutdown without metastasis besides its antitumor immunity.

6. Recommendation

Since the colon can be easily accessed via the rectum opening of the large intestine using an endoscope. Thus, colonoscopy endoscopes could be used to directly deliver PSs drugs (HY and HAHY) to target tumor regions, as well as administer the required wavelength of laser irradiation light to activate a PS drug. So, this form of oncological PDT treatment for CRC tumors is possible.

ACKNOWLEDGEMENTS

We acknowledge the Scientific & Medical Research Center (ZSMRC), Faculty of Medicine, Zagazig University for its support.

Disclosure statement

The authors declare no conflicts of interest, financial or otherwise.

AUTHOR CONTRIBUTIONS

All authors performed the experiments, analyzed the data, interpreted the results of the experiments, and drafted the manuscript.

Ethics statement

All animal experiments were approved by the ZSMRC, Faculty of Medicine, Zagazig University. Animal Research Ethics and were done in accordance with their guidelines for Animal Care.

6. REFERES

1. Wolf, A.M., Fontham, E.T., Church, T.R., Flowers,C.R., Guerra, C.E., LaMonte, S.J., Etzioni, R., McKenna, M.T., Oeffinger, K.C., Shih, Y.C.T. and Walter, L.C. Colorectal cancer screening for average-risk adults: 2018 guideline update from the American Cancer Society. CA: a cancer journal for clinicians, 2018; 68(4): 250-281.
2. Bogaert, J. and Prenen, H. Molecular genetics of colorectal cancer. Ann Gastroenterol, 2014; 27(1): 9–14.
3. Gaston, D. and Giacomantonio, C. Genomic of colorectal cancer In: Arceci GDNBJ, editor. Cancer Genomics. Boston, MA, USA: Academic Press, 2014; 247-264.
4. Rothenberg, M.L., Oza, A.M., Bigelow, R.H., Berlin, J.D., Marshall, J.L., Ramanathan, R.K., Hart, L.L., Gupta, S., Garay, C.A., Burger, B.G., Le Bail, N. and Haller, D.G. Superiority of oxaliplatin and fluorouracil–leucovorin compared with either therapy alone in patients with progressive colorectal cancer after irinotecan and fluorouracil–leucovorin: interim results of a phase III trial. J Clin Oncol, 2003; 21: 2059–2069.
5. Lonardi, S., Sobrero, A., Rosati, G., Di Bartolomeo, M., Ronzoni, M., Aprile, G., et al. (2016). Phase III trial comparing 3–6 months of adjuvant FOLFOX4/XELOX in stage II–III colon cancer: safety and compliance in the TOSCA trial, Ann Oncol, 2016; 27(11): 2074–2081.
6. Pachman, D.R., Qin, R., Seisler, D.K., Smith, E.M., Beutler, A.S., Ta, L.E., Lafky, J.M., et al. Clinical course of oxaliplatin-induced neuropathy: results from the randomized phase III trial N08CB (Alliance). J Clin Oncol, 2015; 33(30): 3416–3422.
7. Pallis, A.G., Fortpied, C., Wedding, U., Van Nes, M.C., Penninckx, B., Ring, A., Lacombe, D., Monfardini, S., Scalliet, P. and Wildiers, H., EORTC elderly task force position paper: approach to the older cancer patient. European Journal of Cancer, 2010; 46(9): 1502-1513.
8. Yang, Z.R., Liu, M., Peng, X.L., Lei, X.F., Zhang, J.X. and Dong, W.G. Noscapine induces mitochondria-mediated apoptosis in human colon cancer cells in vivo and in vitro. Biochem Bioph Res Co, 2012; 421: 627-633.
9. Barathan, M., Mariappan, V., Shankar, E.M., Abdullah, B.J.J., Goh, K.L. and Vadivelu, J. Hypericin-photodynamic therapy leads to interleukin-6 secretion by HEPG2 cells and their apoptosis via recruitment of BH-3 interacting-domain death agonist and caspases. Cell Death Dis., 2013; 27: e697.
10. Olivo, M, Bhuvaneswari, R., Lucky, Ss., Dendukuri, N. and Soo-Ping-Thong, P. Targeted therapy of cancer using photodynamic therapy in combination with multi-facted anti-tumor modalities. Pharmaceuticals, 2010; 3: 1507-1529.
11. Agostinis, P., Berg, K., Cengel, K,A., Foster, Th., Girotti, A,W., Gollnick, S.O., Hahn, S.M., Hamblin, M.R., Juzeniene, A., Kessel, D., Korbelik, M., Moan, J., Mroz, P., Nowis, D., Piette, J., Wilson, B.C. and Golab, J. Photodynamic therapy of cancer: An update. Ca Cancer J Clin, 2011; 61: 250-81.
12. Dolmans, D.E., Fukumura, D. and Jain, R.K. "Photodynamic therapy for cancer," Nat. Rev. Cancer, 2003; 35: 380–387.
13. Castano, A.P., Mroz, P., and Hamblin, M.R. "Photodynamic therapy and anti-tumour immunity," Nat. Rev. Cancer, 2006; 67: 535–545.
14. Agostinis, P., Vantieghem, A., Merlevede, W. and de Witte, P.A. Hypericin in cancer treatment: more light on the way. Int. J. Biochem. Cell Biol, 2002; 34: 221–241.
15. Fox, E., Murphy, R.F., McCully, C.L. and Adamson, P.C. Plasma pharmacokinetics and cerebrospinal fluid penetration of hypericin in nonhuman primates, Cancer Chemother. Pharmacol, 2001; 47: 41–44.
16. Ritz, R., Wein, H.T., Dietz, K., Schenk, M., Roser, F., Tatagiba, M. et al. Photodynamic therapy with glioma with hypericin: Comprehen sive in vitro study in glioblastoma cell lines. Int J Oncol, 2007; 30: 659-66.
17. Oleinick, N.L., Morris, R.L. and Belichenko, L. The role of apoptosis in response to photodynamic therapy: what, where, why and how. Phoyochem Photobiol Sci, 2002; 1: 1-21.

18. Hostanska, K., Reichling, J., Bommer, S., Weber, M. and Sallera, R. Hyperforin a constituent of St John's wort (Hypericum perforatum L.) extract induces apoptosis by triggering activation of caspases and with hypericin synergistically exerts cytotoxicity towards human malignant cell lines. Eur. J. Pharm. Biopharm, 2003; 56: 121–132.
19. Soussi, T. P53 alterations in human cancer: more questions than answers, Oncogene, 2007; 26: 2145-2156.
20. Vousden, K.H. and Lane, D.P. P53 in health and disease, Nat. Rev. Mol. Cell Biol, 2007; 8: 275–283.
21. Mikes, J., Kleban, J., Sackova, V., Horvath, V., Jamborova, E., Vaculova, A., Kozubık, A., Hofmanova, J. and Fedorocko, P. Necrosis predominates in the cell death of human colon adenocarcinoma HT-29 cells treated under variable conditions of photodynamic therapy with hypericin, Photochem. Photobiol. Sci, 2007; 6: 758–766.
22. Delaey, E., Vandenbogaerde, A., Merlevede, W. and De Witte, P. Photocytotoxicity of hypericin in normoxic and hypoxic conditions. J. Photochem. Photobiol, B., 2000; 56: 19–24.
23. Yang, C.C., Chu, K.C. and Yeh, W.M. "The expression of vascular endothelial growth factor in transitional cell carcinoma of urinary bladder is correlated with cancer progression," Semin Urol. Oncol, 2004; 221: 1–6.
24. Marchal, S., Fadloun, A., Maugain, E., D'Hallewin, M.A., Guillemin, F. and Bezdetnaya, L. Necrotic and apoptotic features of cell death in response to Foscan photosensitization of HT29 monolayer and multicell spheroids, Biochem. Pharmacol, 2005; 69: 1167–1176.
25. Sasano, H. and Suzuki, T. "Pathological evaluation of angiogenesis in human tumor," Biomed. Pharmacother, 2005; 59(2): S334–336.
26. Yee, K.K., Soo, K.C. and Olivo, M. "Anti-angiogenic effects of hypericin-photodynamic therapy in combination with Celebrex in the treatment of human nasopharyngeal carcinoma," Int. J. Mol. Med, 2005; 166: 993–1002.
27. Ferrario, A. and Gomer, C.J. Avastin enhances photodynamic therapy treatment of Kaposi's sarcoma in a mouse tumor model. J Environ Pathol Toxicol Oncol, 2006; 25: 251-259.
28. Bhuvaneswari, R., Gan, Y.Y., Yee, K.L., Soo, K.C. and Olivo, M. Effect of hypericin-mediated photodynamic therapy on the expression of vascular endothelial growth factor in human nasopharyngeal carcinoma. Int. J. Mol. Med, 2007; 20: 421–428.
29. Harper, C.E., Patel, B.B., Wang, J., Eltoum, I.A. and Lamartiniere, C.A. "Epigallocatechin-3- gallate suppresses early stage, but not late stage prostate cancer in TRAMP mice: mechanisms of action," Prostate, 2007; 67: 141576–1589.
30. Sakamoto, Y., Terashita, N., Muraguchi, T., et al. Effects of epigallocatechin-3-gallate (EGCG) on A549 lung cancer tumor growth and angiogenesis, Biosci. Biotechnol. Biochem, 2013; 77: 17991803.
31. Braicu, C., Gherman, C.D., Irimie, A., et al. Epigallocatechin-3-Gallate (EGCG) inhibits cell proliferation and migratory behaviour of triple negative breast cancer cells, J. Nanosci. Nanotechnol, 2013; 13: 632–637.
32. Lambert, J.D. and Yang, C.S. Mechanisms of cancer prevention by tea constituents. J. Nutr, 2013; 133: 3262S–3267S.
33. Du, G.J., Zhang, Z., Wen, X.D., et al. Epigallocatechin gallate (EGCG) is the most effective cancer chemopreventive polyphenol in green tea. Nutrients, 2012; 4: 1679-1691.
34. Johar, D., Roth, J.C., Bay, G.H., Walker, J.N., Kroczak, T.J. and Los, M. Inflammatory response, reactive oxygen species, programmed (necrotic- like and apoptotic) cell death and cancer. Rocz Akad Med Bialymst, 2004; 49: 31-39.
35. Koon, H-K., Lo, K-W., Leung, K-N., Lung, M.L., Chang, CC-K., Wong, RN- S., et al. Photodynamic therapy-mediated modulation of inflammatory cytokine production by Epstein-Barr virus-infected nasopharyngeal carcinoma cells. Cell Mol Immunol, 2010; 7.
36. Ritz, R., Roser, F., Radomski, N., Strauss, W.S.L., Tatagiba, M., Gharabaghi, A. Subcellular colocalization of hypericin with respect to endoplasmic reticulum and Golgi apparatus in glioblastoma cells. Anticancer Res, 2008; 28: 2033-2038.
37. Amer, A.M., Falk, H. and Tran, H.T. The dissociation and tautomerization equilibria of hypericin: alkyl protected hydroxyl derivatives. Monatshefte für Chemie / Chemical Monthly, 1998; 129(12): 1237-1244.
38. Menshawi, B.S., Fayad, W., Mahmoud, K., Hallouty, S.M., Manawaty, M.E., Olofsson, M.H. and Linder, S. Screening of natural products for Therapeutic activity against solid tumors. *Indian Journal of Experimental Biology*, 2010; 48(3): 258-264.
39. Rajput, A., Martin, D.S., Rose, R., Beko, A., Levea, C., Sharratt, E., Mazurchuk, R., Hoffman, R.M., Brattain, M.G. and Wang, J. "Characterization of HCT116 Human Colon Cancer Cells in an Orthotopic Model". Journal of Surgical Research, 2008; 147(2): 276–281.
40. Chen, B., Roskams, T., Xu, Y., Agostinis, P. and DeWitte, P.A. Photodynamic therapy with hypericin induces vascular damage and apoptosis in the RIF-1 mouse tumor model. Int J Cancer, 2002; 98: 284-290.
41. Cavarga, I., Brezáni, P., Cekanová-Figurová, M., Solár, P., Fedorocko, P. and Miskovský, P. Photodynamic therapy of murine fibrosarcoma with topical and systemic administration of hypericin. Phytomedicine, 2001; 8: 325–330.
42. Bannerman, B., Xu, L., Jones, M., Tsu, C., Yu, J., Hales, P., Monbaliu, J., Fleming, P., Dick, L., Manfredi, M. and Claiborne, C. Preclinical evaluation of the antitumor activity of bortezomib in

combination with vitamin C or with epigallocatechin gallate, a component of green tea. Cancer chemotherapy and pharmacology, 2011; 68(5): 1145-1154.
43. Robinson, S.M., Mann, D.A., Manas, D.M., Oakley, F., Mann, J. and White, S.A. The potential contribution of tumour-related factors to the development of FOLFOX-induced sinusoidal obstruction syndrome. British journal of cancer, 2013; 109(9): 2396.
44. Assefa, Z., Vantieghem, A., Declercq, W., Vandenabeele, P., Vandenheede, J.R., Merlevede, W., de Witte, P. and Agostinis, P. The activation of the c-Jun N-terminal kinase and p38 mitogen-activated protein kinase signaling pathways protects HeLa cells from apoptosis following photodynamic therapy with hypericin. Journal of Biological Chemistry, 1999; 274(13): 8788-8796.
45. Livak, K.J. and Schmittgen, T.D. Analysis of relative gene expression data using real-time quantitative PCR and the 2− ΔΔCT method. methods, 2001; 25(4): 402-408.
46. Wang, X., Liu, Y., Dai, L., Liu, Q., Jia, L., Wang, H., An, L., Jing, X., Liu, M., Li, P. and Cheng, Z. Foxp3 downregulation in NSCLC mediates epithelial-mesenchymal transition via NF-κB signaling. Oncology reports, 2016; 36(4): 2282-2288.
47. Jang, D.H., Song, D.H., Chang, E.J. and Jeon, J.Y. Anti-inflammatory and lymphangiogenetic effects of low-level laser therapy on lymphedema in an experimental mouse tail model. Lasers Med Sci, 2016; 31: 289–296.
48. Chang, H.H., Miaw, S.C., Tseng, W., Sun, Y.W., Liu, C.C., Tsao, H.W. and Ho, I.C. PTPN22 Modulates Macrophage Polarization and Susceptibility to Dextran Sulfate Sodium–Induced Colitis. J Immunol, 2013; 191(5): 2134-2143.
49. Funk, L.H., Hackett, A.R., Bunge, M.B. and Lee, J.K. Tumor necrosis factor superfamily member APRIL contributes to fibrotic scar formation after spinal cord injury. J Neuroinflammation, 2016; 13: 87.
50. Suvarna, K.S., Layton, C. and Bancroft, J.D. eds., Bancroft's Theory and Practice of Histological Techniques E-Book. Elsevier Health Sciences, 2013; 323- 326.
51. Mármol, I., Sánchez-de-Diego, C., Pradilla Dieste, A., et al. Colorectal carcinoma: a general overview and future perspectives in colorectal cancer. Int J Mol Sci, 2017; 18(1): E197.
52. Kuebler, J.P., Wieand, H.S., O'Connell, M.J., Smith, R.E., Colangelo, L.H., Yothers, G., Petrelli, N.J., et al. Oxaliplatin combined with weekly bolus Fluorouracil and leucovorin as surgical adjuvant chemotherapy for stage II and III colon cancer: results from NSABP C-07. J Clin Oncol, 2007; 25(16): 2198– 2204.
53. Andre, T., Boni, C., Navarro, M., Tabernero, J., Hickish, T., Topham, C., Bonetti, A., Clingan, P., Bridgewater, J., Rivera, F., de Gramont, A. Improved overall survival with oxaliplatin, fluorouracil, and leucovorin as adjuvant treatment in stage II or III colon cancer in the MOSAIC trial. J Clin Oncol, 2009; 27(19): 3109–3116.
54. Mroz, P., Hashmi, J.T., Huang, Y.Y., Lange, N. and Hamblin, M.R. Stimulation of anti-tumor immunity by photodynamic therapy. Expert Rev Clin Immunol, 2011; 7(1): 75-91.
55. Sačková, V., Fedoročko, P., Szllardiová, B., Mikeš, J. and Kleban, J. Hypericin-induced photocytotoxicity is connected with G2/M arrest in HT-29 and S-phase arrest in U937 cells. J Photoch Photobio B, 2006; 82: 1285-1291.
56. Sanovic, R., Verwanger, T., Hartl, A. and Krammer, B. Low dose hypericin-PDT induces complete tumor regression in BALB/c mice bearing CT26 colon carcinoma. Photodiagn Photodyn Ther, 2011; 8: 291-296.
57. Paszkoa, E., Ehrhardt, C., Senge, M.O., Kelleher, D.P., Reynolds, J.V. Nanodrug applications in photodynamic therapy. Photodiagnosis Photodyn, 2011; 8: 14–29.
58. Yoo, J.O. and Ha, K.S. New insights into the mechanisms for photodynamic therapy-induced cancer cell death. Int Rev Cel Mol Bio, 2012; 295: 139– 174.
59. Kruger, C.A. and Abrahamse, H. Targeted Photodynamic Therapy as Potential Treatment Modality for the Eradication of Colon Cancer. Kruger, Cherie & Abrahamse, Heidi. (2019). Targeted Photodynamic Therapy as Potential Treatment Modality for the Eradication of Colon Cancer. 10.5772/Intechopen, 2018; 84760.
60. Blank, M., Kostenich, G., Lavie, G., Kimel, S., Keisari, Y. and Orenstein, A. Wavelength-dependent properties of photodynamic therapy using hypericin in vitro and in an animal model. Photochem. Photobiol, 2002; 76: 335–340.
61. Mikes, J., Koval, J., Jendzelovsky, R., Sackova, V., Uhrinova, I., Kello, M., et al. The role of P53 in the efficiency of photodynaic therapy with hypericin and subsequent long-term survival of colon cancer cells. Photochem. Photobiol. Sci, 2009; 8: 1558-1567.
62. Süloğlu, A.K., Selmanoğlu, G. and Akay, M.T. Alterations in dysadherin expression and F- actin reorganization: a possible mechanism of hypericin-mediated photodynamic therapy in colon adenocarcinoma cells. Cytotechnology, 2015; 67: 1–20.
63. Plaetzer, K., Krammer, B., Berlanda, J., Berr, F. and Kiesslich, T. Photophysics and photochemistry of photodynamic therapy: fundamental aspects. Lasers Med Sci, 2009; 24(2): 59-68.
64. Van Golen, R.F., Reiniers, M.J., Olthof, P.B., van Gulik, T.M. and Hege, M. Sterile inflammation in hepatic ischemia/reperfusion injury: Present concepts and potential therapeutics. Journal of

Gastroenterology and Hepatology, 2013; 28: 394–400.
65. Turrens, J.F. Mitochondrial formation of reactive oxygen species. J Physiol, 2003; 552(Pt 2): 335-344.
66. Liu, T., Wu, L.Y., Choi, J.K. and Berkman, C.E. Targeted photodynamic therapy for prostate cancer: Inducing apoptosis via activation of the caspase-8/-3 cascade pathway. Int J Oncol, 2010; 1: 777–784.
67. Du, H., Bay, B., Mahendran, R. and Olivo, M. Hypericin-mediated photodynamic therapy elicits differential interleukin-6 response in nasopharyngeal cancer. Cancer Lett, 2006; 235: 202-208.
68. Fisher, A.M., Ferrario, A., Rucker, N., Zhang, S. and Gomer, C.J. Photodynamic therapy sensitivity is not altered in human tumor cells after abrogation of p53 function, Cancer Res, 1999; 59: 331- 335.
69. Tong, Z., Singh, G. and Rainbow, A.J. The role of the p53 tumor suppressor in the response of human cells to photofrin-mediated photodynamic therapy. Photochem Photobiol, 2000; 71: 201–210.
70. Hajri, A., Wack, S., Meyer, C., Smith, M.K., Leberquier, C., Kedinger, M. and Aprahamian, M. In Vitro and In Vivo Efficacy of Photofrin® and Pheophorbide a, a Bacteriochlorin, in Photodynamic Therapy of Colonic Cancer Cells. Photochemistry and photobiology, 2002; 75(2): 140-148.
71. Jiang, F., Zhang, X., Kalkanis, S.N., Zhang, Z., Yang, H., Katakowski, M., Hong, X., Zheng, X., Zhu, Z. and Chopp, M., Combination therapy with antiangiogenic treatment and photodynamic therapy for the nude mouse bearing U87 glioblastoma. Photochemistry and photobiology, 2008; 84(1): 128-137.
72. Chen, B., Pogue, B. W., Hoopes, P. J. and Hasan, T. Combining vascular and cellular targeting regimens enhances the efficacy of photodynamic therapy. International Journal of Radiation Oncology Biology Physics, 2005; 61: 1216–1226.
73. Chen, B. and de Witte, P.A. Photodynamic therapy efficacy and tissue distribution of hypericin in a mouse P388 lymphoma tumor model. Cancer Lett, 2000; 150: 111-117.
74. Ferrario, A., Von-Tiehl, K., Wong, S., Luna, M. and Gomer, C.J. Cyclooxygenase-2 inhibitor treatment enhances photodynamic therapy- mediated tumor response. Cancer Research, 2002; 62: 3956–3961.
75. Makowski, M., Grzela, T., Niderla, J., ŁAzarczyk, M., Mróz, P., Kopeé, M., Legat, M., Strusińska, K., Koziak, K., Nowis, D., Mrówka, P., Wasik, M., Jakóbisiak, M., & Golab, J. Inhibition of cyclooxygenase-2 indirectly potentiates antitumor effects of photodynamic therapy in mice. Clinical Cancer Research, 2003; 9: 5417–5422.
76. Ferrario, A., Fisher, A. M., Rucker, N., & Gomer, C. J. Celecoxib and NS-398 enhance photodynamic therapy by increasing in vitro apoptosis and decreasing in vivo inflammatory and angiogenic factors Cancer Research, 2005; 65: 9473– 9478.
77. Ferrario, A., Lim, S., Xu, F., Luna, M., Gaffney, K. J., Petasis, N.A., Schönthal, A. H. and Gomer, C. J. Enhancement of photodynamic therapy by 2,5-dimethyl celecoxib, a non-cyclooxygenase-2 inhibitor analog of celecoxib. Cancer Letters, 2011; 304: 33–40.
78. Bhuvaneswari, R., Yuen, G.Y., Chee, S.K. and Olivo, M. Antiangiogenesis agents avastin and erbitux enhance the efficacy of photodynamic therapy in a murine bladder tumor model. Lasers Surg. Med, 2011; 43: 651–662.
79. Siddiqui, I.A., Malik, A., Adhami, V.M., et al. Green tea polyphenol EGCG sensitizes human prostate carcinoma LNCaP cells to TRAIL-mediated apoptosis and synergistically inhibits biomarkers associated with angiogenesis and metastasis, Oncogene, 2008; 27: 2055–2063.
80. Hönicke, A.S., Ender, S.A. and Radons, J. Combined administration of EGCG and IL-1 receptor antagonist efficiently downregulates IL-1-induced tumorigenic factors in U-2 OS human osteosarcoma cells. Int. J. Oncol, 2012; 41: 753–758.
81. Kwak, T.W., Kim, D.H., Chung, C.W., et al Synergistic Anticancer Effects of Vorinostat and Epigallocatechin-3-Gallate against HuCC-T1 Human Cholangiocarcinoma Cells, Evid. Based Complementary Altern. Med, 2013: 18515.
82. Wu, H., Xin, Y., Xu, C., et al. (2012). Capecitabine combined with (-)- epigallocatechin-3-gallate inhibits angiogenesis and tumor growth in nude mice with gastric cancer xenografts, Exp. Ther. Med, 3: 650–654.
83. Fingar, V.H. Vascular effects of photodynamic therapy. Journal of Clinical Laser Medicine and Surgery, 1996; 14: 323–328.
84. Ochsner, M. Photophysical and photobiological processes in the photodynamic therapy of tumours. Journal of Photochemistry and Photobiology B, 1997; 39: 1-18.
85. Gollnick, S.O., Liu, X., Owczarczak, B., Musser, D.A. and Henderson, B.W., Altered expression of interleukin 6 and interleukin 10 as a result of photodynamic therapy in vivo. Cancer research, 1997; 57(18): 3904-3909.
86. Korbelik, M., and Cecic, I. Contribution of myeloid and lymphoid host cells to the curative outcome of mouse sarcoma treatment by photodynamic therapy. Cancer Letters, 1999; 137: 91–98.
87. Moor, A.C. Signaling pathways in cell death and survival after photodynamic therapy. J Photochem Photobiol B, 2000; 57: 1–13.
88. Gollnick, S.O., Evans, S.S., Baumann, H., Owczarczak, B., Maier, P., Vaughan, L. et al. Role of cytokines in photodynamic therapy- induced local and systemic inflammation. Br J Cancer, 2003; 88: 1772–1779.
89. Gabay, C. Interleukin-6 and chronic inflammation. Arthritis Res Ther, 2006; 8: S3.

90. Kabingu, E.N. Photodynamic therapy mechanisms of anti-tumor immunity. State University of New York at Buffalo, 2007.
91. Thong, P.S.P., Ong, K.W., Goh, N.S.G., Kho, K.W., Manivasager, V., Bhuvaneswari, R., Olivo, M. and Soo, K.C. Photodynamic-therapy- activated immune response against distant untreated tumours in recurrent angiosarcoma. The lancet oncology, 2007; 8(10): 950-952.
92. Trisciuoglio, L. and Bianchi, M.E. Several nuclear events during apoptosis depend on caspase3 activation but do not constitute a common pathway. PLoS One, 2009; 4: e6234.
93. Firczuk, M., Nowis, D. and Gołąb, J., PDT- induced inflammatory and host responses. Photochemical & Photobiological Sciences, 2011; 10(5): 653-663.
94. Zhao, H., Xing, D. and Chen, Q. New insights of mitochondria reactive oxygen species generation and cell apoptosis induced by low dose photodynamic therapy. Eur J Cancer, 2011; 47: 2750– 2761.
95. He, Y., Ge, H. and Li, S. Haematoporphyrin based photodynamic therapy combined with hyperthermia provided effective therapeutic vaccine effect against colon cancer growth in mice. Int J Med Sci, 2012; 9(8): 627–633.